

Hydrate dissolution influence on the Young's modulus of cement pastes

S. Kamali & M. Moranville

LMT, ENS-Cachan, 61 avenue du Président Wilson, 94230 Cachan, France

E. Garboczi

National Institute of Standards and Technology, Gaithersburg, Maryland 20899 USA

S. Prené

EDF-R&D/Les Renardières, Ecuelles, F-77818 Moret sur Loing Cedex, France

B. Gérard

OXAND S.A., 36 bis, avenue Franklin Roosevelt, 77210 Avon, France

ABSTRACT: Leaching of concrete by water may severely damage structures like radioactive waste depositories or water supply stations. This paper presents the influence of water leaching on the mechanical properties of cement pastes. The NIST microstructure model CEMHYD3D and elastic model ELAS3D were used to quantify the effect of the dissolution of cement hydrates like calcium hydroxide (CH), monosulphoaluminate (AFm) and ettringite (AFt), on the Young's modulus. The results clearly indicate the important impact of calcium hydroxide dissolution on the decrease of this parameter. Calcium hydroxide leaching can reduce the Young's modulus by more than 50 %, depending on the initial calcium hydroxide content. Different cement pastes were simulated to investigate the effect of two parameters: water to cement ratio and silica fume addition. An empirical equation relating the capillary porosity to the Young's modulus was developed.

Keywords: cement, hydrates, microstructure, leaching, dissolution, portlandite, monosulfoaluminate, ettringite, porosity, elastic moduli

1 INTRODUCTION

Leaching by water is a degradation mechanism for concrete structures such as dams and tunnels. This phenomenon becomes more alarming for structures designed to last several hundred of years, which is the case for radioactive waste depositories. Several investigations on old concrete structures have shown that water deteriorates concrete (Badouix 2000) and increases its porosity (Fujiwara et al. 1992). The phenomenon of leaching has been studied in several laboratories to identify its consequences on the physical and mechanical properties of cement-based materials. In contact with a reservoir of water with an ionic composition different from that of the cement paste pore solution (typically lower), various ions, and particularly calcium and hydroxyl ions, diffuse from the pore solution towards the water reservoir. These transfers involve a chemical disequilibrium and consequently a dissolution or precipitation of solid phases (Adenot & Buil 1992). Following the ranking of their solubility products, portlandite (CH) is the first hydrate to be dissolved followed

by monosulphoaluminate (AFm) and then ettringite (AFt). Lastly, C-S-H is decalcified and transformed into a silica gel with minimal mechanical properties. Thus, the leached zone is characterized by a succession of dissolution-precipitation fronts between zones in chemical equilibrium, as shown in Fig. 1. The dissolution of the hydrates in cement-based materials involves an increase in porosity (Tognazzi 1998, Matte & Moranville 1999), a decrease in the elastic modulus and in the compressive strength (Carde 1996, Gérard 1998, Kamali 1999 & Le Bellégo 2001), an increase in material ductility (Carde 1996), a reduction in the fracture energy (Le Bellégo 2001), and a reduction in the friction coefficient as obtained by a triaxial compression test under drained conditions (Heukamp 2001).

The elastic or Young's modulus is one of the most important and critical properties of concrete material and structural mechanical design. The quantification of the reduction in this property due to the dissolution of one or more hydrates is not easy to measure. However, the NIST 3D microstructure models are well adapted for this

type of study. These models have been used to quantify the dissolution effect of portlandite (CH), ettringite (AFt) and monosulfoaluminate (AFm), on the elastic modulus. The modelling has then been validated using one experimental result. Different cement pastes were simulated to study effect of the water-to-cement ratio, w/c, and silica fume addition. Empirical formulas were developed to relate the decrease of the elastic modulus to the increase in capillary porosity during leaching.

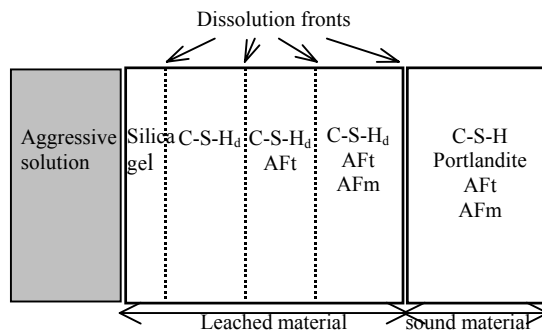


Figure 1. Leaching zones in a portland cement paste (w/c=0.4) leached by pure water at pH=7 and T=20 °C, according to Adenot (1992); C-S-H_d = decalcified C-S-H.

2. MODELLING THE LEACHING EFFECT ON THE YOUNG'S MODULUS

2.1. Methodology

To evaluate the consequences of the leaching of CH, AFm and AFt on the cement paste elastic modulus, we used two NIST models: CEMHYD3D and ELAS3D. The first one is a three-dimensional cement hydration and microstructure development modelling package. The second one is a finite element linear elastic program developed for computing the linear elastic properties of random materials whose microstructure has been stored in a 2D or 3D digital image. Several steps were followed:

1. The first step consisted in building the three-dimensional microstructure of the unleached paste by using the CEMHYD3D program. This program has been previously described in detail (Bentz 1997). The cubic hydration volume is $100^3 \mu\text{m}^3$ or 10^6 voxel elements. Among other results, this program computes the hydrate volume fractions and capillary porosity.

2. The second step consisted in simulating the leaching of CH, AFt and AFm by replacing the pixels representing these phases by those of water. The hydrate volume fractions and the capillary porosity of the unleached and leached material were provided by the program. This simulated

leaching was done globally, in order to see material response, and so would not set up leached zones, as in Fig. 1, since there was not a surface where leaching started. The CEMHYD3D model has periodic boundary conditions (Bentz 1997).

3. The third step consisted in computing the Young's modulus of the unleached and leached microstructures using the ELAS3D program. This code is described in detail elsewhere (Garboczi 1998). The microstructures obtained in steps 1 and/or 2 were used as input data for the program (Garboczi 1998). The elastic moduli of each voxel were defined by its corresponding phase.

2.2. Application and validation of the modelling

In order to check the relevance of this modelling, a comparison with an experimental result is necessary. Based on physico-chemical characterization and compression test results, Carde (1996) found that total dissolution of CH caused a reduction of 55 % in the Young's modulus of portland cement paste with w/c= 0.5.

The different modelling steps described in section 2.1 were applied to Carde's cement paste and the simulated value of the elastic modulus reduction after CH leaching was compared to the experimental one. The mineralogical composition of the cements studied is presented in Table 1. These values were used in the CEMHYD3D model. Table 2 gives the elastic modulus and Poisson's ratio values of the principal phases used in the ELAS3D code (1 % to 2 % uncertainty in all values). The used water phase properties are the bulk modulus (K) equal to 2.2 GPa and shear modulus (G) equal to 0.0 GPa (Lide 1997).

Table 1. Mineralogical composition of Carde's Portland cement using Bogue method (% weight content) (Carde 1996).

C ₃ S	C ₂ S	C ₃ A	C ₄ AF	Gypsum
57.4 %	14.7 %	8.2 %	9.2 %	5.4 %

Table 2. Young's modulus, E, and Poisson's ratio values of the principal phases used in modelling.

Phases	E (GPa)	ν	References
C ₃ S	117.6	0.314	Boumiz et al. 1997
C ₂ S	117.6	0.314	
C ₃ A	117.6	0.314	
C ₄ AF	117.6	0.314	
Gypsum	45.7	0.33	Choy et al. 1979, Bhalla 1984
Portlandite	42.3	0.324	Monteiro & Chang 1995
C-S-H	22.4	0.25	Damidot et al. 2003
C-S-H _{pozz}	22.4	0.25	
Afm	42.3	0.324	
Aft	22.4	0.25	
Empty porosity	0	0	

The model values of the Young's modulus of unleached and leached cement pastes are given in Table 3. If the random hydration and leaching simulations were run several times, there would only be about a 1 % or lower value of the standard deviation in these moduli. The results show the important effect of CH dissolution on the decrease of the elastic modulus. The effect of the dissolution of the sulfoaluminates, AFm and AFt, appears less important than does dissolution of CH, with the dissolution of AFm being the least important in reduction of the Young's modulus. A reduction of 49 % was found after only CH leaching. This model value is in good agreement with the experimental value of 51 %.

Table 3. Hydrate dissolution effect on the Young's modulus – numerical results using ELAS3D.

	Young's Modulus	
	Gpa	% of unleached cement paste
Unleached	19.0	100
CH dissolution	9.8	51
CH and AFm dissolution	9.8	51
CH, AFm and AFt dissolution	8.3	43

3. INFLUENCE OF WATER-TO-CEMENT RATIO AND SILICA FUME ADDITION ON LEACHED MATERIAL PROPERTIES

To investigate the effects of water-to-cement ratio (w/c) and silica fume addition on the decrease of the Young's modulus due to leaching, six cement pastes were simulated: three w/c ratios (0.5, 0.4, 0.25) for two industrial cements, ordinary portland cement (CEM I) and blended portland cement with 7.7 % silica fume content (CEM II/A). Cement CEMII/A is made by adding silica fume at the cement plant to CEM I as a mass replacement for CEM I. So therefore the "c" in "w/c" represents the weight of the cement CEM II, a mixture of Portland cement and silica fume. These cement pastes were previously studied by Kamali (2003). Their formulations are given in Table 4.

Table 4. Composition of the six cement pastes.

Paste n°	Cement type	w/c	Silica fume content %
1	Portland (CEM I)	0.5	0 %
2	Portland (CEM I)	0.4	0 %
3	Portland (CEM I)	0.25	0 %
4	CEM II/A	0.5	7.7 %
5	CEM II/A	0.4	7.7 %
6	CEM II/A	0.25	7.7 %

3.1. Numerical simulation

The microstructures of the six cement pastes were simulated using the CEMHYD3D program. This model operates by a sequence of steps : dissolution, random-walker diffusion of the mobile agents, and reaction between colliding pixels. One complete sequence is called a cycle of hydration. The simulated microstructures were representative of the real microstructures, in that the hydration cycle number was fixed in such a way that the simulated CH volume fraction was chosen to be as close as possible to that found in experiment (Kamali 2003). First, simulations of 5000 hydration cycles were performed. Then, as shown in Figure 2, a cycle number was chosen so that the numerical CH content evolution agreed within two or three significant figures with the experimental CH content value. Table 5 presents the number of cycles identified for each cement paste and a comparison between simulated CH content values and those measured experimentally. In paste number 6, the 5000 cycles of hydration used, as well as model inaccuracies in simulating the effect of silica fume, made it not possible to obtain such close agreement with the CH content. A unit cell 100 μm in size was used for all the simulations.

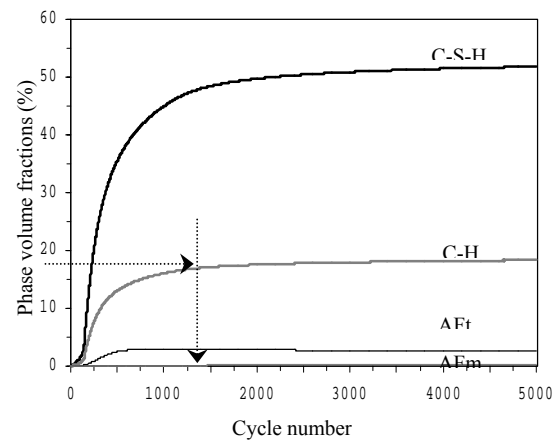
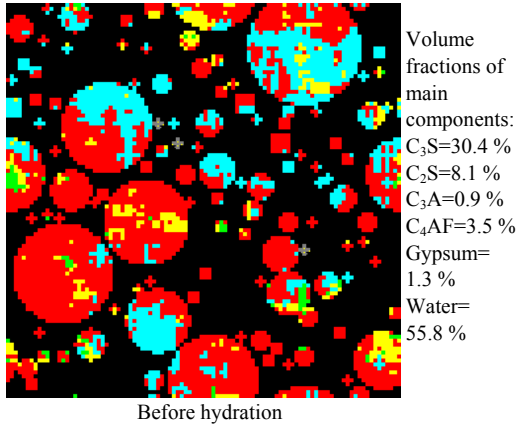
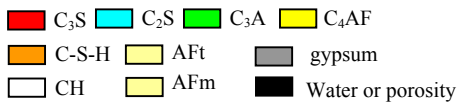
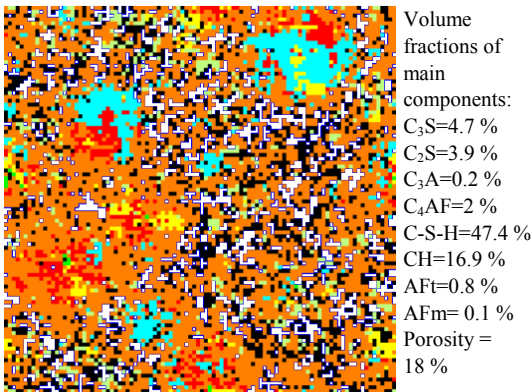


Figure 2: Evolution of the principal hydrate volume fractions with the number of hydration cycles (for portland cement paste at w/c=0.4).

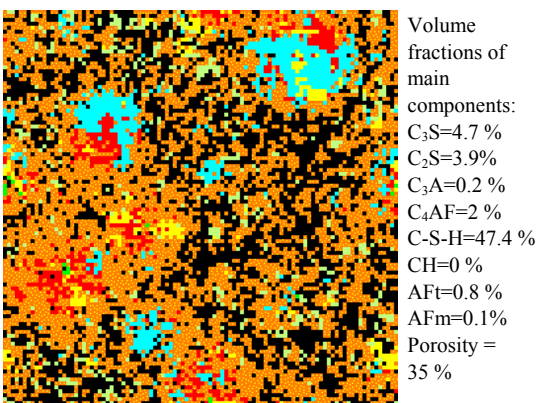
Once the 3D microstructures of unleached hydrated cement pastes were built, the leaching of CH, AFm and AFt were simulated. Figure 3 presents 2D images obtained from 3D numerical microstructures of Portland cement paste with w/c = 0.4, before hydration, after hydration and after CH dissolution. It is clearly shown that the dissolution of CH (shown in white) increases the porosity (shown in black).



Before hydration



After 1378 hydration cycles



After CH dissolution

Figure 3. 2D images obtained from 3D microstructures of portland cement paste with w/c=0.4 before hydration, after hydration and after CH dissolution. The images are 100 μm in width.

Table 5. Cycle number and numerical and measured CH content.

Paste n°	Cement type	w/c	Cycle number	CH mass content (%) Model	CH mass content (%) Experiment
1	CEM I	0.5	2351	20	20
2	CEM I	0.4	1378	20	20
3	CEM I	0.25	1319	16	16
4	CEM II/A	0.5	1947	13	13
5	CEM II/A	0.4	1378	13	13
6	CEM II/A	0.25	5000	9	10

3.2. Leaching influence on capillary porosity

The volume fractions of the main phases and the capillary porosity given by the model for the six cement pastes are presented in Table 6. The results are in good agreement with what is already known concerning the increase of capillary porosity with the water-to-cement ratio and the reduction in CH content with silica fume addition (Huang & Feldman 1985, Regourd 1987).

Table 6. Volume fractions of principal hydrates and capillary porosity model value.

w/c =	Volume fractions in %					
	CEM I paste			CEM II/A paste		
	0.5	0.4	0.25	0.5	0.4	0.25
CH	16.4	16.9	15.7	10.5	10.8	8.5
C-S-H	47.3	47.4	42.1	38.6	38.8	32.7
C-S-H _{pouzz}	-	-	-	10.8	10.9	12.4
AFt	2.4	2.8	2.9	2.7	2.3	2.9
AFm	0.16	0.14	0.3	0.4	0.4	1
Porosity (%)	23.7	18.3	11.0	24.0	18.4	11.1

Previously, Bentz et al. (1992) have shown the important effect of CH dissolution on the porous network percolation of tricalcium silicate cement pastes. We studied the influence of the total dissolution of CH and also of AFm and AFt on the increase in the capillary porosity for the six cement pastes. The model values of capillary porosity of the unleached, and the CH, AFm and Aft-leached cement pastes are given in Table 7. The results show an important capillary porosity increase after total CH dissolution for the different pastes. To evaluate the effect of the CH, AFm and AFt dissolution, we calculated the capillary porosity ratios after and before leaching. As shown in Fig. 4, the total CH dissolution has a very important effect on the increase in the capillary porosity and particularly for pastes with lower water-to-cement ratios. The total dissolution of AFm and AFt also contributes to the increase in capillary porosity, but in a much smaller way, due to the fact that their volume fractions in the unleached cement paste are

much lower, i.e. 0.16 % AFm and 2.4 % AFt compared to 16.4 % CH in the CEMI at w/c = 0.5. For the different systems, with and without silica fume, the capillary porosity due to hydrate dissolution increases with water-to-cement ratio.

Table 7: Capillary porosity values for the different cement pastes before and after CH, AFm and AFt dissolution - CEMHYD3D results.

w/c =	Capillary porosity p_{cap} , %					
	CEM I paste			CEM II/A paste		
	0.5	0.4	0.25	0.5	0.4	0.25
unleached	23.7	18.3	11.0	24.0	18.4	11.1
without CH	40.1	35.1	26.7	34.5	29.2	19.6
without CH and AFm	40.3	35.3	27.0	34.9	29.5	20.6
without CH, AFm and AFt	42.7	38.1	30.0	37.0	30.6	21.5

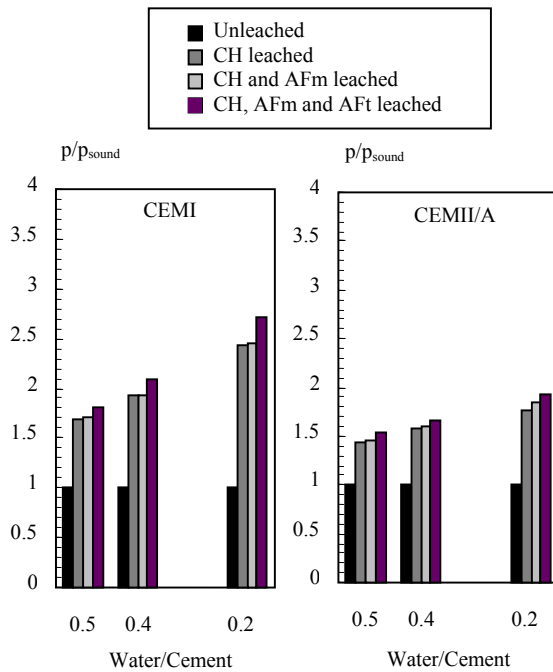


Figure 4. Leaching effect of CH, AFm and AFt on the increase of capillary porosity.

In the study of transfer phenomena, the connected capillary porosity is an important and critical parameter to be taken into account. It is known that the entire capillary porosity system is not totally connected. The connectivity depends on the capillary porosity value. For high values, beyond 0.4, the capillary porosity is almost fully connected. Thus, the dissolution of hydrates can strongly increase the connected capillary porosity fraction (fraction of total sample volume). It is

important to remember that this study can predict properties of fully leached areas in the cement paste, but it is not made to simulate the progression of the leaching front. The connected capillary porosity fraction was computed for the six cement pastes before and after leaching of hydrates, using CEMHYD3D. The model values are given in Fig. 5. The results indicate that CH dissolution significantly increases the connected porosity fraction, connecting previously isolated pores. This effect is highlighted in the cement pastes with w/c = 0.25. The AFm and AFt dissolution contributed slightly to the connectivity of the porous network because their original volume fraction in unleached cement pastes was lower.

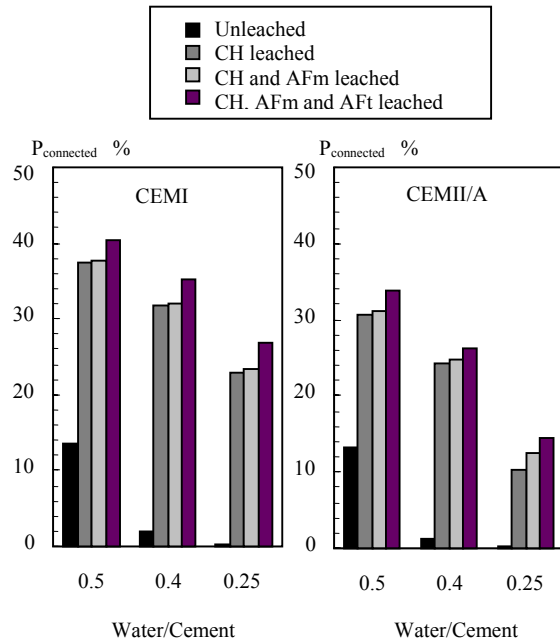


Figure 5: Leaching effect of CH, AFm and AFt on the increase of the connected capillary porosity fraction (expressed as a fraction of total sample volume).

3.3. Influence of leaching on the Young's modulus

The two main goals of the modelling study on the six leached cement pastes were to quantify the dissolution effect of CH, AFm and AFt on the value of the elastic modulus, and develop a simple equation to relate the reduction in the Young's modulus to the increase in the capillary porosity. Table 8 summarizes the model values of Young's modulus for the unleached and leached cement pastes. Results clearly show an important decrease of this parameter in the leached cement pastes. The

reduction rate depends on the water-to-cement ratio and silica fume addition.

Table 8. Young's modulus, E , value for the various cement pastes according to the rate of degradation – numerical results obtained by ELAS3D program.

w/c =	E (GPa)					
	CEM I paste			CEM II/A paste		
	0.5	0.4	0.25	0.5	0.4	0.25
unleached	18.6	23.0	32.7	17.8	21.9	30.8
without CH	8.7	11.9	19.0	11.6	14.9	23.9
without CH and AFm	8.6	11.9	18.7	11.5	14.7	23.1
without CH, AFm and AFt	7.8	10.8	17.0	10.7	14.3	22.6

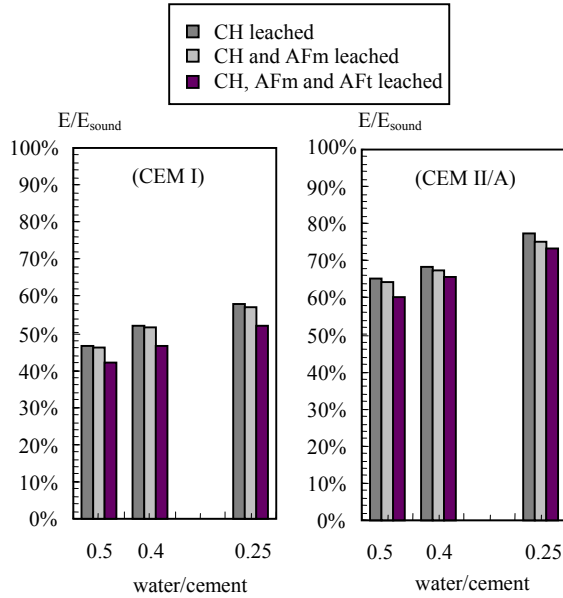


Figure 6. Dissolution effect of CH, AFm and AFt on the Young's modulus decrease of the six cement pastes.

To further quantify the effect of the hydrate dissolution on the reduction in the Young's modulus, we calculated the leached-to-unleached cement paste elastic modulus ratios, as shown in Fig. 6. The results clearly indicate the important effect of portlandite dissolution in the decrease of this parameter value. This reduction increases with the water-to-cement ratio.

For the two other hydrates, AFm and AFt, whose original volume fraction was low (see Table 6), their dissolution caused a much lower decrease in the Young's modulus of the different cement pastes. The system with silica fume has a higher residual elastic modulus value. It is due to the lower initial content of CH, which in turn is due to

the pozzolanic reaction of the silica fume. Much less CH originally means that much less CH could be leached. In all the cases, the value of Young's modulus found after leaching decreases as w/c increases.

4. EMPIRICAL FORMULA RELATING THE DECREASE IN THE YOUNG MODULUS TO THE INCREASE OF THE CAPILLARY POROSITY

Different empirical equations relating Young's modulus to porosity exist in the literature. However, the porosity considered depends on the experimental methods used to determine it. In this paper, we propose a new formula adapted for capillary porosity given by the CEMHYD3D model. A plot of the Young's modulus model values obtained from the different simulations, versus total capillary porosity, is provided in Fig. 7. The following equation relating Young's modulus to capillary porosity is fitted to the different model values.

$$E = 46.03 \cdot (1 - p_{cap})^{3.16} \quad (1)$$

where E = cement paste Young's modulus (GPa);
 p_{cap} = cement paste capillary porosity.

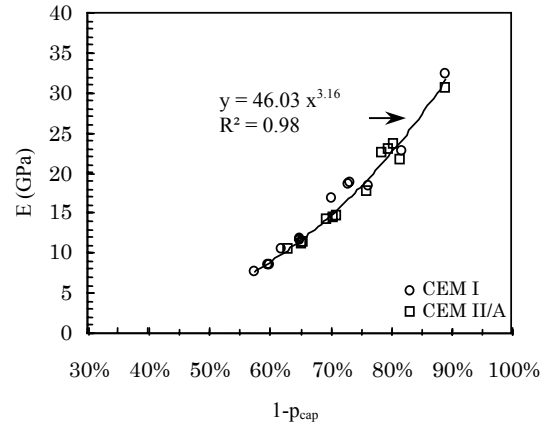


Figure 7. Numerical simulations results for the different cement pastes, leached and non-leached.

Based on Equation 1, the reduction of the Young's modulus due to leaching can be expressed as a function of unleached and leached cement paste capillary porosity as shown in Equation 2:

$$\frac{E}{E_0} = \left(\frac{1 - p_{cap}}{1 - p_{cap0}} \right)^{3.16} \quad (2)$$

where E = leached cement paste Young's modulus (GPa); E_o = unleached cement paste Young's modulus (GPa); p_{capo} = unleached cement paste capillary porosity; p_{cap} = leached cement paste capillary porosity.

5. CONCLUSION

Using the CEMHYD3D and ELAS3D microstructure and property models, the leaching from cement paste of the phases CH, AFm, and Aft was numerically simulated. Leaching effects on capillary porosity, connected capillary porosity fraction, and Young's modulus were computed and analysed for six cements, at three different water-to-cement ratios and with and without 7.7 % silica fume addition. The results clearly show that CH dissolution strongly increases capillary porosity and its connected fraction and significantly decreases the Young's modulus value. A reduction of more than 50 % in Young's modulus was found, in good agreement with experiment. These increase and reduction rates depend on the initial CH content and consequently on water-to-cement ratio and silica fume addition. The system with silica fume had a higher residual elastic modulus value due to the lower initial CH content. For the six cement pastes, the fractional reduction in elastic modulus increases with the water-to-cement ratio. As far as the two other hydrates, AFm and Aft, are concerned, their dissolution causes a much lower increase in capillary porosity and decrease in Young's modulus because their initial volume fraction is much lower than that of CH. Finally, an empirical equation relating elastic modulus to capillary porosity was developed using the numerical results.

6. REFERENCES

- ADENOT, F., BUIL M. 1992. Modeling of the corrosion of the cement paste by de-ionized water. *Cement and Concrete Research* 22: 489-496.
- BADOUIX, F. 2000. Modélisation de l'altération à long terme des bétons : prise en compte de la carbonatation. LMT-ENS de Cachan, France, PhD Thesis.
- BENTZ, D.P. & GARBOCZI, E.J. 1992. Modelling the leaching of calcium hydroxide from cement paste : effects on pore space percolation and diffusivity. *Materials and Structures* 25: 523-533.
- BENTZ, D.P. 1997. Three-Dimensional Computer simulation of Portland Cement Hydration and Microstructure Development. *Journal of American Ceramic Society* 80 (1): 3-21.
- BHALLA, A.S., COOK, W.R., HEARMON, R.F.S., JERPHAGNON, J., KURTZ, S.K., LIU, S.T., NELSON, D.F., OUDAR, J.-L. 1984. Landolt-Bornstein: Numerical data and functional relationships in science and technology new series. Group III: Crystal and solid state physics. Volume 18 (Supplement to volume III/11). Elastic, Piezoelectric, Pyroelectric, Piezooptic, Electrooptic Constants, and nonlinear dielectric susceptibilities of crystals. Editors K.-H. Kellwege and A.M. Hellwege. Springer-Verlag Berlin.
- BOUMIZ, A., SORRENTINO, D., VERNET, C., COHEN TENOUDJI, F. 1997. Modelling the development of the elastic moduli as a function of the degree of hydration of cement pastes and mortars. *Proceedings 13 of the 2nd RILEM Workshop on Hydration and Setting: Why does cement set? An interdisciplinary approach*, Edited by Nonat A. RILEM, Dijon, France.
- CARDE, C. 1996. Caractérisation et modélisation de l'altération des propriétés mécaniques due à la lixiviation des matériaux cimentaires. INSA de Toulouse, France, PhD Thesis.
- CHOY, M.M., COOK, W.R., HEARMON, R.F.S., JAFF, J., JERPHAGNON, J., KURTZ, S.K., LIU, S.T., NELSON, D.F. 1979. Landolt-Bornstein: Numerical data and functional relationships in science and technology new series. Group III: Crystal and solid state physics. Volume 11 (Revised and extended edition of volume III/1 and III/2). Elastic, Piezoelectric, Pyroelectric, Piezooptic, Electrooptic constants, and nonlinear dielectric susceptibilities of crystals. Editors K.-H. Kellwege and A.M. Hellwege. Springer-Verlag Berlin.
- DAMIDOT, D., VELEZ, K., SORRENTINO, F. 2003. Characterisation of interstitial transition zone (ITZ) of high performance cement by nanoindentation technique. presented in the 11th International Congress on the Chemistry of Cement, Durban.
- FUJIWARA, Y., MARUYA, T., OWAKI, E. 1992. Degradation of concrete buried in soil with saline ground water. *Nuclear Engineering and Design* 138: 143-150 (North-Holland).
- GARBOCZI, E.J. 1998. Finite element and finite difference programs for computing the linear electric and elastic properties of digital images of random materials. NISTIR 6269, U.S. Department of Commerce/NIST.
- GÉRARD, B., PIJAUDIER-CABOT G., LABORDERIE C. 1998. Coupled diffusion-damage modelling and the implications on failure due to strain localisation. *International Journal of Solids and Structures*, Vol. 35, 31-32: 4107-4120.
- HEUKAMP, P.H., ULM, F.J., GERMAINE, J.T. 2001. Mechanical properties of calcium leached cement pastes : triaxial stress and the influence of the pore pressure. *Cement and Concrete Research* 31(5): 767-774.
- HUANG, C. Y., FELDMAN, R.F. 1985. Hydration reactions in Portland cement – silica fume blends. *Cement and Concrete Research* 15: 585.
- KAMALI, S. 1999. Identification de la loi de comportement mécanique d'un mortier lixivié par du nitrate d'ammonium. Ecole Normale Supérieure de Cachan, France, Rapport de DEA.
- KAMALI, S. 2003. Comportement et simulation des matériaux cimentaires en environnements agressifs : lixiviation et température. LMT-ENS de Cachan, France, PhD Thesis.
- LE BELLEGO, C. 2001. Couplage chimie mécanique dans les structures en béton armé attaquées par l'eau – Etude expérimentale et analyse numérique. LMT-ENS de Cachan, France, PhD Thesis.
- LIDE, D.R. 1997. CRC Handbook of Chemistry and Physics. 78th Edition. CRC Press Boca Raton, Florida. P. 6-127.
- MATTE, V., MORANVILLE M. 1999. Durability of reactive powder composites : influence of silica fume on the leaching properties of very low water/binder pastes. *Cement and Concrete Composites* 21: 1-9.
- MONTEIRO, P.J.M., CHANG, C.T. 1995. The elastic moduli of calcium hydroxide. *Cement and Concrete Research* 25: 1605-1609.

- REGOURD, M. 1987. Microstructure of cement blends containing fly ash, silica fume, slag and fillers. *Materials Research Symposium Proceeding on Microstrutural Development During Hydration of Cement, Materials Research Societ,y 85: 187-200.*
- TOGNAZZI, C. 1998. Couplage fissuration - dégradation chimique dans les matériaux cimentaires : caractérisation et modélisation. INSA de Toulouse, France, PhD Thesis.